*Chem. Chem. Technol., 2023,*
*Vol. 17, No. 2, pp. 386–396*

**Chemical Technology**

# OPTIMIZED DESIGN AND FABRICATION OF POLYETHYLENE GLYCOL 1000/POLYAMIDE 6 (PEG1000/PA6) NANOFIBERS FOR PHASE CHANGE MATERIALS (PCMS) APPLICATION

*Fariba Karimian[1], Gholamreza Karimi[1,✉], Mohammad Khorram[1], Reihaneh Daraeinejad[1], Mahnaz M. Abdi[1,✉]*

https://doi.org/10.23939/chcht17.02.386

**Abstract.** Ultrafine phase change nanofibers based on polyethylene glycol 1000 (PEG1000) as phase change material (PCM) and polyamide 6 (PA6) as a supporting material were prepared in a systematic manner planned by the Design-Expert® software using the uniaxial electrospinning. Research surface methodology (RSM) was carried out to optimize the parameters and conditions leading to minimize the fiber diameter. The effect of PEG content, applied voltage, needle gauge, and flow rate on the fiber characteristics was studied by a central composite design (CCD). The minimum diameter of nanofibers was predicted by a quadratic model to be 64.33 nm and the actual fibers diameter prepared under optimal condition showed a very low relative standard error (RSE). It was shown that the PEG/PA6 mass ratio has the dominant effect on the fibers diameter. The results from FTIR and FE-SEM images confirmed well encapsulated PEG in PA6 and no leakage and morphology alterations were observed after heating tests. To further investigate morphological structure and the quality of PEG1000 encapsulation in PA6 matrices, the composite fibers underwent a solvent treatment using ethanol. The results proposed a new innovative method to control operational electrospinning conditions for encapsulating phase change materials in polymer matrices which is very important in thermal energy saving/retrieving applications.

**Keywords:** electrospinning, phase change material (PCM), response surface methodology (RSM), polyethylene glycol, polyamide 6.

## 1. Introduction

The energy crisis and high cost of fossil fuels, as well as environmental pollution have promoted research activities in alternative and renewable energy sources.[1,2] Many researches have been conducted to find materials and methods for developing new energy sources, however, the growing demand for energy is still challenging.[3] One of the important energy conversion methods is to use thermal energy storage materials to reduce price and increase storage capacity in small temperature intervals.[4-6] Among the thermal energy storage (TES) forms, latent heat storage (LHS) using phase change materials (PCMs) are an effective solution to reduce energy consumption in different applications *via* storing and retrieving thermal energy as a latent heat.[5-9] High heat storage density, isothermal nature of storage process, small temperature variation from the storage to retrieval, low cost, chemical stability, *etc.*, have made PCMs a very good candidate for many energy-related applications such as a solar energy utilization, space and water heating, low energy buildings, thermo-regulating fibers and smart textiles, medical applications, space crafts, engines cooling, air conditioning systems, and thermal insulation for functional fibers.[2,10,11]

Despite extensive applications and advantages, PCMs suffer from possible leakages into the surrounding during the phase change process.[1] Thus they should be placed in special containers which may result in excessive thermal resistance and operating costs.[5,12] To eliminate this problem, encapsulating PCMs supporting by polymers are suggested.[4,5,13] Therefore, form-stable (shape stabilized) phase change materials are an attractive solution in this field.[1,14]

Phase change fibers (PCFs) are one of the most important groups of form-stable PCMs due to their promising applications in the smart fabrics and cloths. Electrospinning as a convenient, simple and low cost method has been extensively applied for fabricating ultrafine fibers and form-stable PCMs.[5,7,14] Since the introduction of electrospinning by Formhals in 1930, it has been the versatile technique to produce nanofibers with diameters ranging from several micrometers to several nanometers, using a huge variety of materials.[15-17] Ultrafine size, high surface-

[1] Department of Chemical Engineering, Shiraz University, Shiraz 7134851154, Iran
✉ *ghkarimi@shirazu.ac.ir, karimi1342@gmail.com; mahnaz131@gmail.com*

to-volume ratio, excellent thermal performance, light weight and multi-scaled porous structure are some of the remarkable electrospun fibers advantages.[6,18] Various form-stable electrospun fibers with embedded PCMs with controllable morphologies, and properties *via* electrospinning technique have been successively reported. McCann *et al.*[19] succeeded in creating ultrafine phase change fibers with a long-chain hydrocarbons core and $TiO_2$-PVP shell. They used the melt coaxial electrospinning and presented a new method for PCMs encapsulation. Chen *et al.*[20] synthesized composite fibers of lauric acid, myristic acid, palmitic acid, and stearic acid each separately with polyethylene terephthalate matrix by using the uniaxial electrospinning. These composite fibers showed desirable thermal properties. In another effort they also fabricated ultrafine electrospun fibers based on polyethylene glycol and poly (D,L-lactide) blends for thermal energy storage application. The fibers showed the enhanced morphology and reliable phase change behavior. It also presented the complete encapsulation of polyethylene glycol by poly(D,L-lactide) matrix.[12] In an initiative study, Rocio Perez *et al.*[21] used electrospinning of dodecane and zein (a maize protein) to fabricate the thermo-regulating smart food packaging. They compared the uniaxial and coaxial electrospinning methods of encapsulation.

The factors that affect the electrospinning process are classified as solution properties, electrospinning parameters, and environmental parameters. Solution properties included viscosity, polymer and solvent concentration, surface tension, and solution conductivity. The electrospinning parameters comprised applied voltage, flow rate, needle diameter, and distance between the needle and the collector. The environmental parameters such as humidity, temperature, and atmosphere pressure are also important factors which affected the electrospinning process.[22] In most of the reported studies in this field, the electrospinning operating conditions were not systematically studied. The objective of the present study is to investigate the electrospinning process in a more systematic manner and to provide a model for predicting the characteristics of composite nanofibers by using RSM.

Changing one factor at a time (OFAT) is a conventional method of optimization, which study only the effect of specific parameter alone and is a material and time-consuming technique.[23,24] On the contrary, response surface methodology is a mathematical and statistical technique that evaluates the effects of multiple parameters, alone or in combination, in response. This method is based on fitting a polynomial equation to the experimental data and is able to reduce the number of experimental sets.[24-26] Polyethylene glycol (PEG) is a typical solid-liquid PCM with exceptional characteristics such as a low vapor pressure, non-corrosivity, non-toxicity, chemical and thermal stability, relatively large enthalpies and wide range of a molecular weight,[10,27,28] which is successively used as a latent heat storage component in the form-stable PCMs. In the present research as PCM we used polyethylene glycol with an average *Mw* of 1000 (PEG1000). Many polymers such as polylactic acid (PLA),[12] polyvinylidene difluoride (PVDF),[29,30] polyamide 6 (PA6),[31,32] and polyvinylpyrrolidone (PVP)[33] were used as the fibrous supporting matrix to encapsulate PEG.

Polyamide 6 (PA6) is also a famous semi-crystalline polymer offering the high strength and toughness, low coefficient of friction, and superior resistance to a wide spectrum of chemicals that has been used as a supporting matrix.[31,32] It is an appropriate polymer for fabricating a form-stable electrospun fiber for encapsulating PEG because its melting point is much higher than that of PEG and it can prevent the leakage of molten PEG at temperatures above PEG melting point.[13]

In the current study the ultrafine phase change nanofibers were prepared based on PEG1000 as the phase change material (PCMs) and PA6as the supporting material. The set of experiments was designed by the Design-Expert® software using the uniaxial electrospinning. The main objective was to study the effect of multiple parameters (applied voltage, solution flow rate, PEG/PA6 mass ratio and needle gauge) on the fiber's diameter and to identify a good fitted model of the experimental data using CCD for fabrication ofPEG-PA6 fibers at optimized conditions predicted by software. The distribution and encapsulation of PEG in PA6 matrices were investigated through the solvent treatment and a heat treatment procedure was conducted to check the form-stable characteristics of the electrospun fibers.

## 2. Experimental

### 2.1. Materials

Polyethylene glycol with an average *Mw* of 1000 (PEG1000) and the melting point range of 308–324 K was purchased from DaeJung (Korea). The pellets of polyamide 6 (PA6, *Mw*=10032, m.p.483 K) were supplied by Sigma-Aldrich (United States). The 85% formic acid was obtained from Sharlau (Spain).

### 2.2. Methods and Characterization

For all experiments, PA6 in the formic acid solution (12 % w/v) was used as the original solution. Different amounts of PEG were added into the PA6 solution to make various PEG/PA6 mass ratio solutions. The mixtures were then put in an ultrasonic bath for 4 h to achieve a homogenous electrospinning solution. The prepared solutions were loaded into 20 mL plastic syringes with blunt-end stainless steel needles. Electrospinning process

was carried out by using a high voltage power supply (Highvoltage-35-OC, Fanavaran Nano Meghias, Iran), a syringe pump (SP1000HOM, Fanavaran Nano Meghias, Iran) and an aluminum flat sheet as the collector. During electrospinning process, the loaded syringe was placed horizontally in the syringe pump and a positive high voltage applied to the needle tip. The distance between the needle tip and the collector was fixed at 12 cm. All experiments were performed at room temperature.

The thermal properties of samples were studied by differential scanning calorimetry (DSC) technique (DSC PT10 Platinum series, Germany, resolution 0.125 mW at RT, temperature accuracy ±0.2 K). To study the thermal energy storage performance of the fibers, the heating/cooling curves of the samples were also determined using two incubators (MMM group, Incucell and Friocell, Germany) as heat sinks. The cold and hot water bath temperatures were adjusted at 283 K and 333 K, respectively. Five grams' fibers of pure PA, PEG, and PEG/PA composite (mass ratio of 50:100) were placed in a plastic veneers prior placing in cold or hot water bath.

The FTIR analysis of PEG/PA6 nanofiber composites, pristine PEG, and PA6 pellets were conducted using a PERKIN-ELMER (RX1) infrared spectrophotometer before and after heat treatment in the wavenumber range of 400–4000 $cm^{-1}$. A MIRA//TESCAN field-emission scanning electron microscope field emission scanning electron microscopy (FE-SEM) was employed to evaluate morphologies of the electrospun fiber composites at an acceleration voltage of 15 kV under low vacuum. All samples were gold plated to avoid charge accumulations. The diameter of the electrospun fibers was calculated by means of the Adobe Photoshop CS6 software from SEM images in their original magnification, at least fifty cases in each sample. It is very important for the prepared nanofiber-PCM composites to maintain their structures and chemical compositions when exposed to a temperature higher than the PCM melting point. In other words, the amount of PCM leakage from the composite should be minimal. To asses this feature, nanofiber composites were placed in a constant temperature oven at 343 K for various times, *e.g.*, 0.5, 1, 2, and 5 h and the weight changes of composites were measured carefully before and after each stage. After 5 h heat treatment, the nanofibers morphologies were characterized by SEM and FTIR. To further investigate the effect of solvent on the morphological structure of the fibers (*e.g.*, PEG dispersions), the composite fibers were immersed in ethanol for 1 h and dried at room temperature and then the structure of the fibers was examined by SEM.

## 2.3. Statistical Analysis

Four-factor-five-level central composite design (CCD) was applied to perform a parametric study in this work. The effects of applied voltage, solution flow rate, PEG-PA6 mass ratio and needle gauge on fibers diameter were investigated. The number of experiments is determined by CCD as

$$N = k^2 + 2k + C_p, \quad (1)$$

where $k$ is the number of factors and $C_p$ is the center point replicate number.

In the present study, the number of independent variables is 4 and hence 30 experiments ($N$) were designed for 6 repetitions in the central point experiment. High and low levels of each variable were coded as $+\alpha$ and $-\alpha$, respectively and the center values were coded as zero. The value of $\alpha$ depends on the number of factors involved.[24] The independent variables with their minimum and maximum values and the details of experimental design are listed in Table 1.

In CCD, the response is related to the independent variables by linear and quadratic terms as following:

$$Y = \beta_0 + \sum_{i=1}^{k} \beta_i x_i + \sum_{i=1}^{k} \beta_{ii} x_i^2 + \sum_{i<j}^{k} \beta_{ij} x_i x_j + \varepsilon, \quad (2)$$

where $Y$ is the response; $\beta_0$ is the constant or offset term; $\beta_i$ is the linear coefficient; $\beta_{ii}$ is the quadratic effect coefficient; $\beta_{ij}$ is the coefficient for interaction; $\varepsilon$ represents the statistical error.[34,35] All of the statistic evaluations are obtained from the CCD method in Design-Expert software (trial version 9).

**Table 1.** Variables and their levels employed on the central composite design

| Variable | | Unit | Coded level of variable | | | | |
|---|---|---|---|---|---|---|---|
| | | | -2 | -1 | 0 | +1 | 2 |
| A | Voltage | kV | 15.00 | 16.75 | 18.50 | 20.25 | 22.00 |
| B | Flow rate | mL/h | 0.50 | 1.00 | 1.50 | 2.00 | 2.50 |
| C | PEG/PA6(mass ratio) | w/w | 50:100 | 100:100 | 150:100 | 200:100 | 250:100 |
| D | Needle gauge | | 14 | 16 | 18 | 20 | 22 |

# 3. Results and Discussion

## 3.1. Analysis of Experimental Design

Studying the combined effect of four independent variables (applied voltage, flow rate, PEG: PA6 mass ratio and needle gauge) on the fibers diameter was one of the main purposes for this study. Hence by using CCD and performing 30 designed experiments, the data were fitted to different models (linear, two factorial, quadratic). Later, analysis of variance (ANOVA) was done to evaluate and find a suitable fitted model of the experimental data and it was shown that the data are most suitably described by a quadratic model with $R^2$ = 0.9388. The experimental data designed by CCD and the actual average fiber diameters are presented in Table 2.

As can be seen from Fig. 1, there is a linear correlation between the predicted and experimental values and they are distributed almost close together. The model coefficient of determination ($R^2$) was 0.9518, which implied that the model perfectly fitted the data and the regression model is valid.

Table 3 shows ANOVA of the model. The computed $F$ value of the model (16.43) shows that the model is significant, and there is only a 0.34 % chance that this large $F$ value of the model could happen due to noise.

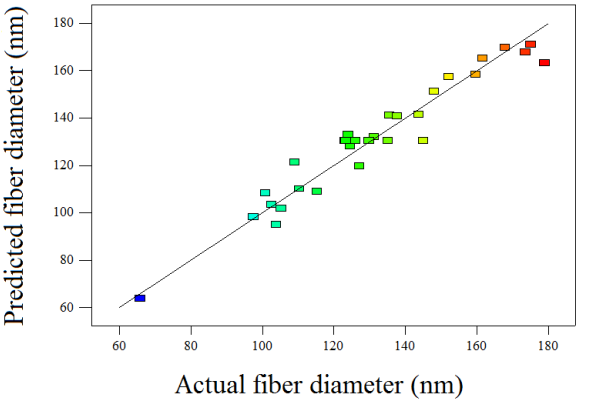


**Fig. 1.** Correlation of the predicted values *versus* actual responses

**Table 2.** Central composite design (CCD) matrix and actual fiber diameter for the fabrication of PEG/PA6 composite nanofiber

| Exp. No. | A, kV | B, mL/h | C, w/w | D | Average fiber diameter, nm |
|---|---|---|---|---|---|
| 1 | 0 | 0 | 0 | 0 | 123.10 |
| 2 | 2 | 0 | 0 | 0 | 143.67 |
| 3 | 1 | -1 | 1 | -1 | 173.63 |
| 4 | 0 | 0 | 0 | 0 | 123.14 |
| 5 | 1 | -1 | -1 | 1 | 102.60 |
| 6 | 0 | 2 | 0 | 0 | 137.70 |
| 7 | 0 | -2 | 0 | 0 | 159.70 |
| 8 | 1 | -1 | -1 | -1 | 109.00 |
| 9 | -1 | 1 | -1 | 1 | 100.98 |
| 10 | 0 | 0 | 0 | 14 | 125.07 |
| 11 | 1 | -1 | 1 | 1 | 175.11 |
| 12 | 1 | 1 | 1 | -1 | 148.10 |
| 13 | 0 | 0 | 2 | 0 | 161.67 |
| 14 | 1 | 1 | 1 | 1 | 152.25 |
| 15 | -1 | -1 | -1 | -1 | 105.27 |
| 16 | 0 | 0 | 0 | 0 | 135.09 |
| 17 | 0 | 0 | 0 | 0 | 129.75 |
| 18 | 0 | 0 | 0 | 22 | 124.05 |
| 19 | 0 | 0 | 0 | 0 | 135.10 |
| 20 | 0 | 0 | 0 | 0 | 167.90 |
| 21 | 0 | 0 | -2 | 0 | 65.84 |
| 22 | 1 | 1 | -1 | 1 | 103.94 |
| 23 | -1 | 1 | 1 | 1 | 179.82 |
| 24 | -1 | -1 | -1 | 1 | 115.33 |
| 25 | 1 | 1 | -1 | -1 | 110.27 |
| 26 | -1 | 1 | 1 | -1 | 131.22 |
| 27 | -2 | 0 | 0 | 0 | 124.61 |
| 28 | 0 | 0 | 0 | 0 | 123.35 |
| 29 | -1 | -1 | 1 | -1 | 13.65 |
| 30 | -1 | 1 | -1 | -1 | 97.54 |

Note: A= Voltage, B=Flow rate, C= PEG: PA6 mass ratio, D=needle gauge

**Table 3.** Analysis of variance (ANOVA) of the model generated for dopamine biosensor fabrication

| Source | Sum of squares | DF | Mean square | *F*-Value | *p*-Value | |
|---|---|---|---|---|---|---|
| Model | 18875.17 | 8 | 2359.40 | 16.43 | <0.0001 | Significant |
| A | 261.74 | 1 | 261.74 | 4.17 | 0.0539 | |
| B | 454.36 | 1 | 454.36 | 0.85 | 0.0137 | |
| C | 15527.42 | 1 | 15527.42 | 247.41 | <0.0001 | Significant |
| D | 274.92 | 1 | 274.92 | 4.38 | 0.0487 | |
| AD | 643.63 | 1 | 643.63 | 10.26 | 0.0043 | |
| CD | 459.23 | 1 | 459.23 | 7.32 | 0.0133 | |
| $B^2$ | 759.72 | 1 | 759.72 | 12.11 | 0.0022 | |
| $C^2$ | 362.11 | 1 | 1062.40 | 362.11 | 0.0256 | |
| Residual | 1317.96 | 21 | 62.76 | | | |
| Lack of fit | 1145.42 | 16 | 71.59 | 2.07 | 0.2154 | |
| Pure error | 172.54 | 5 | 34.51 | | | |
| Corrected Total | 20193.13 | 29 | | | | |
| R-Squared | | | 93.88 | Adequate | 16.706 | |
| Adjusted $R^2$ | | | 88.16 % | Pred.$R^2$ | 72.35 % | |

Note: A= Voltage, B=Flow rate, C= PEG/ PA6 mass ratio, D=needle gauge

The *F*- and *p*-value tests were conducted to investigate the accuracy of the proposed model.[36] The quadratic model was significant for the fibers diameter with the *F*-value of 16.43. The *p*-value < 0.0001 reveals that there is only a probability of 0.01 % of obtaining these results by chance. Values of "Prob > *F*" less than 0.1000 indicates the model terms are significant. From ANOVA analysis shown in Table 3, it is obvious that all linear terms are significant. According to the *p*-value, PEG/PA6 mass ratio(C) has a strong effect in response, while needle gauge (D) and the applied voltage (A) presented weaker effects in response. Among the interaction coefficients terms, the interaction between applied voltage and needle gauge (AD) and also the interaction between PEG/PA6 mass ratio and needle gauge (CD) showed the most significant interaction with the *p*-value of 0.0043 and 0.0133, respectively. It was found that other interactive effects were insignificant.

The coefficient of determination, $R^2$, is 93.88 %, indicating that the data variability was well described by the model. The adjusted determination coefficient (Adj.$R^2$) is also sufficiently high (88.16 %) which indicates that the proposed model is enough significant for fibers diameters response. Furthermore, predicted *R* square (Pred.$R^2$) calculated to be 72.35 demonstrates the applicability of the proposed model to predict the other data's in the range of experimental conditions. The small difference between Adj.$R^2$ and Pred.$R^2$ represents well-fitting proposed model.[35] Another parameter for evaluating the model is the signal-to-noise ratio denoted as "Adequate", a value of which greater than 4 indicates that the proposed model is appropriate for screening, identifying important factors and capable of distinguishing between factors. In the present model the ratio of 16.706 indicates an adequate signal confirming the model which can be used to navigate the design space. Also, the "Lack of Fit *F*-value" of 1.24 implies that this value is insignificant relative to the pure error, so the omitted terms from the model are really unimportant.[25]

Based on the results obtained from ANOVA analysis, the final equations derived to predict the fibers diameter ($D_F$) within the range of experimental operating conditions are presented as Eq.(3):

$$D_F = -398.08688 + 20.76752A - 30.64821B - 0.26715C + 35.02009D - 2.16429AB + 0.020357AC - 1.79821AD - 0.055250BC + 0.71875BD + 0.053187CD + 0.37041A^2 + 19.08750B^2 + 1.58625\,(10)^{-3}\,C^2 - 0.25391D^2 \quad (3)$$

where $D_F$ is fiber diameter, nm; A is applied voltage; B is flow rate; C is PEG/ PA6 mass ratio; and D is needle gauge.

## 3.2. Interactive Effect of Parameters

Fig. 2a demonstrates the combined effect of both needle gauge and PEG/PA6 mass ratio (CD) on the fiber diameter. As shown in the three-dimensional and contour plots in this figure, at a constant needle gauge, the fibers become thicker as PEG content increases. At high PEG concentrations, increasing the needle gauge will result in larger fiber diameters. However, at low PEG concentrations, larger needle gauges, have small influence on the fibers diameter. Fig. 2b shows the simultaneous effects of the applied voltage and needle gauge (AD) on the fiber diameter. As seen from this figure, at low voltages, the fibers diameter increased at larger nozzle gauges however, at high voltages, the fibers diameter decreased when the needle gauge was increased. At small nozzle gauges, a rise in applied voltage will produce thicker fibers while

with larger nozzle gauges' finer fibers are produced as voltage increased.

## 3.3. Optimization

Fabricating nanofibers with minimum diameter is very important in the electrospinning process because the thinner and homogenous fibers create larger surface-to-volume ratios[37] that result in higher heat transfer rate. In the present study, optimization was performed to minimize the response with CCD. A validation test was also done to evaluate the proposed model and the results are listed in Table 4. According to this table, the experimentally measured nanofiber diameters are very close to those predicted by the model suggesting that the empirical model derived from CCD can sufficiently describe the relationship between the independent variables and the response. Low relative standard error (RSE) was found from triplicate experiments which confirmed the validity of the model.

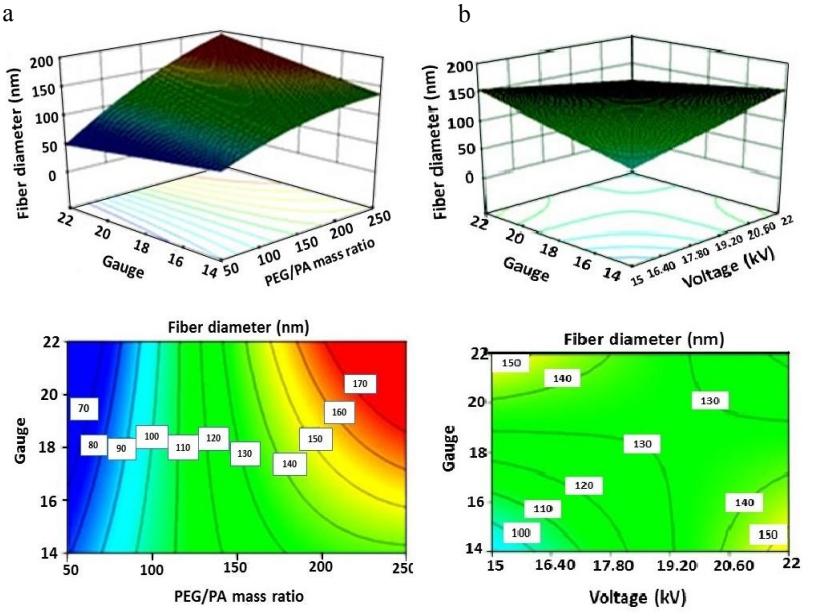


**Fig. 2.** Surface and contour plots for response variable affected by needle gauge and PEG/ PA6 mass ratio (a); by needle gauge and applied voltage (b)

**Table 4.** Optimum operating conditions and validation test

| Optimum value of variables | | | | Response | | |
|---|---|---|---|---|---|---|
| A, kV | B, mL/h | C, w/w | D | Predicted diameter, nm | Experimental diameter, nm | RSE, % |
| 18.50 | 1.50 | 50:100 | 18 | 64.33 | 70.40 | 8.63 |
| | | | | | 68.60 | 6.22 |
| | | | | | 74.80 | 13.99 |

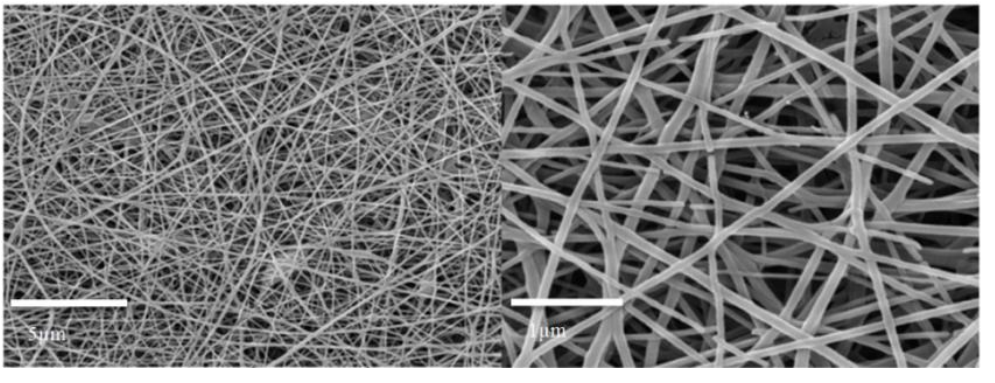

**Fig. 3.** Fibersprepared at optimum condition predicted by software with minimum diameter

The finest fibers and best morphology were obtained by RSM method of optimization for PEG1000/PA6 composite fibers in uniaxial electrospinning. Fig. 3 depicts the morphology of the fibers with the optimum diameter. As evident from the images, the nanofibers are quite uniform with smooth surfaces.

## 3.4. Solvent Treatment Analysis

In order to assess the quality of PEG encapsulation and distribution in PA6 matrix, the produced nanofibers were the solvent treated by ethanol. The experiments were conducted for three kinds of fibers formed at different PEG/PA6 mass ratios of 100:100, 150:100 and 250:100. Nanofiber samples were immersed in ethanol for 1 h to allow PEG dissolution and the amount of PEG removed from the composite fibers is measured. The SEM images of these samples before and after immersion in ethanol are given in Figs. 4a–4c and 4d–4f, respectively. As seen in Figs. 4a-4c, fibers surfaces are smooth and uniform prior to solvent treatment however, after immersion tests, their surfaces become rough and larger pores appeared in the matrices, as is shown in Figs. 4d–4f. These figures confirm the idea of PEG uniform distribution in the PA6 matrices, in which PEG domain was removed from the surface of fibers. This is due to the application of uniaxial electrospinning process, in which phase change materials are scattered uniformly in the polymer matrix. This conclusion is in accordance with previously reported findings.[12,13]

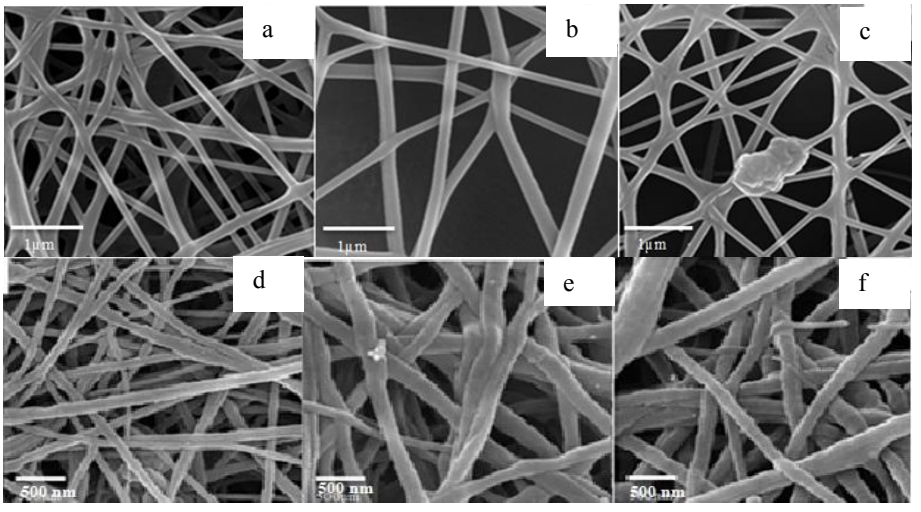


**Fig. 4.** Electrospun composite fibers of PEG/PA before (a,b,c) and after (d,e,f) solvent treatment with mass ratio of 100/100(a,d), 200:100 (b,e) and 250:100(c,f)

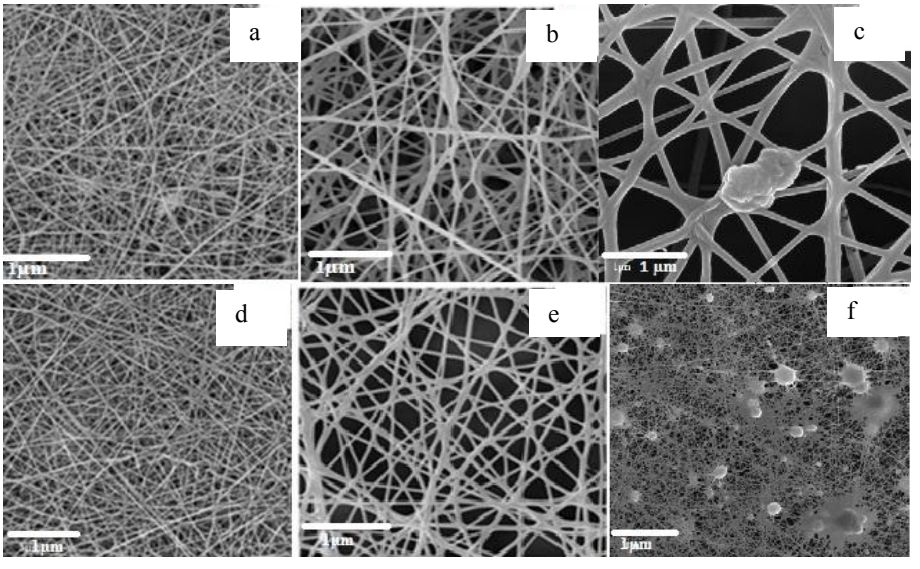


**Fig. 5.** Electrospun composite fibers of PEG/PA before (a,b,c) and after (d,e,f) heat treatment with mass ratio of 100/100 (a,d), 200:100 (b,e) and 250:100 (c,f)

## 3.5. Heat Treatment Study

Another way to check PEG encapsulation in PA6 matrix and form-stable characteristic of the electrospun fibers is the heat treatment. For this purpose, phase change fibers were placed in an oven at 343 K for various time periods of heat treatment (0.5, 1, 2, and 5 h). After 5 h of heat treatment, the mass of the composite fibers was measured, FTIR analysis was conducted, and the fibers morphologies were characterized by SEM.

Experimental results indicated that the mass of composite fibers of PEG/PA6 with 50/100 to 200/100 mass ratio was unchanged after 5 h of heat treatment. This indicates that no PEG leakage occurred from the fibers mats during the heat treatment. This conclusion is consistent with the reported results in the literature.[12,13] However, the composite mats with larger PEG content (250/100), a 5.35 % mass reduction was observed after 8 h of heat treatment, after which the mass remained unchanged.

The morphology of fibers with 50/100 and 100/100 mass ratio and fibers with 200/100 PEG/PA6 mass ratios, before and after heat treatment are presented in Fig. 5. No differences were observed in the fibers morphological structures for fibers with 50/100 to 200/100 PEG/ PA6 mass ratios. However, the morphological structure of PEG/ PA6 fibers prepared from the solution with 250/100 mass ratio showed a huge difference, before and after heat treatment. Some beads and tubercles are observed in the composite before heat treatment caused by the accumulation of excessive polyethylene glycol during the electrospinning process. This fact was also reported in literature.[38] Therefore, mass reduction in the maximum PEG content fibers, caused by PEG leakage due to the presence of many grains and beads in fiber matrices. Fig. 5b presents beads and grains as the leakage and sediment like precipitates between fibers mats after 5 h exposing to the temperature of 343 K. In addition, the FTIR spectra of composites fibers exhibited no changes in nanofibers chemical compositions after exposing to the temperatures higher than PEG melting point confirming the high encapsulation efficiency (Fig. 2b) and is consistent with previous findings.[12,39]

## 3.6. Thermal and Structural Properties

The results obtained from DSC analysis are summarized in Table 5. As seen, the enthalpy values of PEG/PA6 (50/100) nanofibers are lower than PEG and higher than pure PA6 nanofibers, demonstrating the energy of solid-liquid phase transition of the electrospun PEG/PA6 nanofibers increases with the addition of PEG. Moreover, the PEG/PA6 fibers melted earlier than PEG and lasted faster that could be possibly due to the higher thermal conductivity of the encapsulated PEG in the form of stable PCMs.

Fig. 6 compares thermal performance of the produced fibers in terms of the thermal energy storage rate. As seen in this figure, PEG exhibits an obvious and broader temperature plateaus in the phase change area compared to PEG/PA6, showing the characteristic of pure materials. No phase change was observed for PA6 as expected and thermal storage was done just *via* increasing the sample temperature. In order to show phase change of materials during cooling, first the samples were kept in the hot water bath (333 K), and after reaching a stable and constant temperature, they were placed in the cold bath of 283 K.

**Table 5.** Thermophysical properties of PEG, PA, PEG/PA 50:100

| Sample | $T_{onset}$, K | $T_{peak}$, K | $T_{offset}$, K | Enthalpy value, kJ/kg |
|---|---|---|---|---|
| PEG | 308 | 316 | 324 | 197 |
| PA | 475 | 483 | 511 | 1.7 |
| PEG/PA | 287.5 | 312 | 329 | 110 |

Fig. 6b shows the cooling curves. The same trend was observed in cooling curves and PA6 presented a continuous decreasing in temperature with no phase change, while the samples of PEG/PA6 and PEG exhibited temperature plateaus related to a phase change from liquid to solid and temperature remained almost constant. The broader plateaus were also observed for PEG.

Fourier transform infrared spectroscopy is used to investigate the chemical composition and key features of the composites. Fig. 7a indicates the FTIR transmission spectra for pristine PEG and PA6. The spectrum of PEG presented a broad peak at 3450 $cm^{-1}$, which is related to the stretching vibration of O–H bond. The peaks at 2891 and 1466 $cm^{-1}$ are assigned to the stretching vibration of C–H bond and bending vibration of $CH_2$ group (scissoring), respectively. The bands at 1347 and 1242 $cm^{-1}$ are assigned to C–H wagging vibration and C–H twisting vibrations, respectively. Stretching vibration of C–O bond in PEG was also observed at 1250.87, 1116, and 954 $cm^{-1}$. As seen from the PA6 spectrum, peaks at 3304.06 and 1640 $cm^{-1}$ were assigned to the stretching vibrations of N–H and C=O (Amide I), respectively. The peak at 1528 $cm^{-1}$is due to N–H bending vibration and C–N stretching (Amide II) and $CH_2$– stretching was observed at 2937 and 2861 $cm^{-1}$. The specific absorption peak of PA6 appeared at 1485 $cm^{-1}$.[39,40] These results are in accor-

dance with previous findings.[12,38] The results of FTIR spectra for PEG/PA6 nanofiber composites before and after the heat process are displayed in Fig. 7b. As seen from this figure, the spectra of the composite fibers possess all of the individual PEG and PA6 characteristics with no evidence of new absorption peaks which declare no chemical reaction occurred between components, during electrospinning process and also heat treatment process. Moreover, the nanofibers revealed overlapped adsorption bands with lower intensity, which could be due to the interaction between components. Overlapping characteristic peaks of pure PEG at 2891 $cm^{-1}$ and the PA6 peak at 2937 and 2861 $cm^{-1}$ formed a broad band at 2886 $cm^{-1}$ in the nanocomposite spectra. In other words, the overlapping characteristic peaks of pure materials caused the peak broadening at the most wavenumbers.

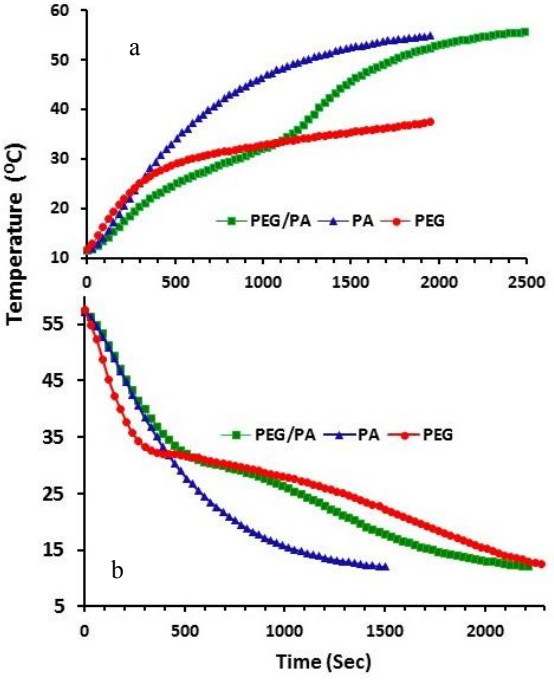


**Fig. 6.** Heating (a) and cooling (b) temperature curves of pure PA6, PEG and the PEG/PA6 with mass ratio of 50/100

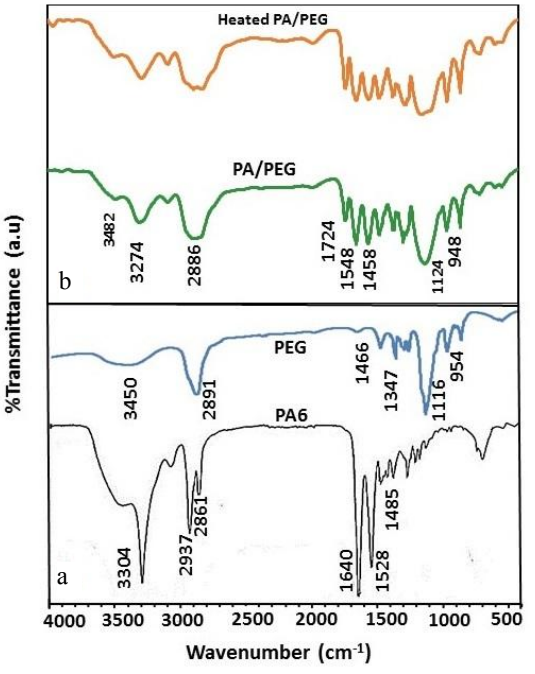


**Fig. 7.** FTIR spectra of pristine PA6 + PEG (a) and PEG/PA6 composite nanofiber (b) before and after heat process

## 4. Conclusions

From Central composite design (CCD), it was found that a quadratic model with $R^2$ of 0.9388 perfectly described data variability for fabricating PEG/PA6 fibers. It was shown that the PEG/PA6 mass ratio has the strongest effect on the fiber diameter, while the needle gauge individually presented less effects in response but in combination with applied voltage displayed the most significant interaction effect. Experimental results indicated that the mass of composite fibers with 50:100 to 200:100 PEG/ PA6 mass ratio was unchanged after 5 h of heat treatment. This indicates that no PEG leakage occurred from the fibers mats during the heat treatment. Thermal analysis confirmed well encapsulated of less amount of PEG in polymer matrices in which no mass changes were observed after heat process but for higher amount of PEG content (250:100), 5.35% mass reduction occurred for its fibers mats through the heat treatment. It is envisioned that PEG/PA6 composite ultrafine nanofibers with 50:100 to 200:100 PEG/PA6 mass ratio as a shape-stabilized composite phase change material, would be the next generation material for thermal regulation and thermal energy storage.

## References

[1] Van Do, C.; Nguyen, T.T.T.; Park, J.S. Fabrication of Polyethylene Glycol/Polyvinylidene Fluoride Core/Shell Nanofibers via Melt Electrospinning and their Characteristics. *Sol. Energy Mater. Sol. Cells* **2012**, *104*, 131-139. https://doi.org/10.1016/j.solmat.2012.04.029
[2] Riffat, S.; Mempouo, B.; Fang, W. Phase Change Material Developments: A Review. *Int. J. Ambient Energy* **2013**, *36*, 102-115. https://doi.org/10.1080/01430750.2013.823106
[3] Iqbal, K.; Sun, D. Development of Thermo-Regulating Polypropylene Fibre Containing Microencapsulated Phase Change Materials. *Renew. Energy* **2014**, *71*, 473-479. https://doi.org/10.1016/j.renene.2014.05.063
[4] Golestaneh, S.I.; Mosallanejad, A.; Karimi, G.; Khorram, M.; Khashi, M. Fabrication and Characterization of Phase Change

Material Composite Fibers with Wide Phase-Transition Temperature Range by Co-Electrospinning Method. *Appl. Energy* **2016**, *182*, 409-417. https://doi.org/10.1016/j.apenergy.2016.08.136
[5] Cai, Y.; Ke, H.; Dong, J.; Wei, Q.; Lin, J.; Zhao, Y.; Song, L.; Hu, Y.; Huang, F.; Gao, W. *et al*. Effects of Nano-$SiO_2$ on Morphology, Thermal Energy Storage, Thermal Stability, and Combustion Properties of Electrospun Lauric Acid/PET Ultrafine Composite Fibers as Form-Stable Phase Change Materials. *Appl. Energy* **2011**, *88*, 2106-2112. https://doi.org/10.1016/j.apenergy.2010.12.071
[6] Cai, Y.; Xu, X.; Gao, C.; Bian, T.; Qiao, H.; Wei, Q. Structural Morphology and Thermal Performance of Composite Phase Change Materials Consisting of Capric Acid Series Fatty Acid Eutectics and Electrospun Polyamide6 Nanofibers for Thermal Energy Storage. *Mater Lett*. **2012**, *89*, 43-46. https://doi.org/10.1016/j.matlet.2012.08.067
[7] Wu, Y.; Chen, C.; Jia, Y.; Wu, J.; Huang, Y.; Wang, L. Review on Electrospun Ultrafine Phase Change Fibers (PCFs) for Thermal Energy Storage. *Appl. Energy* **2018**, *210*, 167-181. https://doi.org/10.1016/j.apenergy.2017.11.001
[8] Sharma, A.; Tyagi, V.V.; Chen, C.R.; Buddhi, D. Review on Thermal Energy Storage with Phase Change Materials and Applications. *Renew. Sustain. Energy Rev*. **2009**, *13*, 318-345. https://doi.org/10.1016/j.rser.2007.10.005
[9] Fallahi, A.; Guldentops, G.; Tao, M.; Granados-Focil, S.; Van Dessel, S. Review on Solid-Solid Phase Change Materials for Thermal Energy Storage: Molecular Structure and Thermal Properties. *Appl. Therm. Eng*. **2017**, *127*, 1427-1441. https://doi.org/10.1016/j.applthermaleng.2017.08.161
[10] Sarier, N.; Onder, E. Organic Phase Change Materials and their Textile Applications: An Overview. *Thermochimica Acta* **2012**, *540*, 7-60. https://doi.org/10.1016/j.tca.2012.04.013
[11] Cai, Y.; Zong, X.; Zhang, J.; Hu, Y.; Wei, Q.; He, G.; Wang, X.; Zhao, Y.; Fong, H. Electrospun Nanofibrous Mats Absorbed with Fatty Acid Eutectics as an Innovative Type of Form-Stable Phase Change Materials for Storage and Retrieval of Thermal Energy. *Sol. Energy Mater. Sol. Cells* **2013**, *109*, 160-168. https://doi.org/10.1016/j.solmat.2012.10.022
[12] Chen, C.; Liu, K.; Wang, H.; Liu, W.; Zhang, H. Morphology and Performances of Electrospun Polyethylene Glycol/Poly(DL-Lactide) Phase Change Ultrafine Fibers for Thermal Energy Storage. *Sol. Energy Mater Sol. Cells* **2013**, *117*, 372-381. https://doi.org/10.1016/j.solmat.2013.07.001
[13] Chalco-Sandoval, W.; Fabra, M.J.; López-Rubio, A.; Lagaron, J.M. Optimization of Solvents for the Encapsulation of a Phase Change Material in Polymeric Matrices by Electro-Hydrodynamic Processing of Interest in Temperature Buffering Food Applications. *Eur. Polym. J*. **2015**, *72*, 23-33. https://doi.org/10.1016/j.eurpolymj.2015.08.033
[14] Na, P.; Widjojo, N.; Sukitpaneenit, P.; Teoh, M.M.; Lipscomb, G.G.; Chung, T.-S.; Lai, J.-Y. Evolution of Polymeric Hollow Fibers as Sustainable Technologies: Past, Present, and Future. *Prog. Polym. Sci*. **2012**, *37*, 1401-1424. https://doi.org/10.1016/j.progpolymsci.2012.01.001
[15] Tort, S.; Acartürk, F. Preparation and Characterization of Electrospun Nanofibers Containing Glutamine. *Carbohydr. Polym*. **2016**, *152*, 802-814. https://doi.org/10.1016/j.carbpol.2016.07.028
[16] Akhtar, M.N.; Sulong, A.B.; Karim, S.A.; Azhari, C.H.; Raza M. R. Evaluation of Thermal, Morphological and Mechanical Properties of PMMA/NaCl/DMF Electrospun Nanofibers: An Investigation Through Surface Methodology Approach. *Iran. Polym. J*. **2015**, *24*, 1025-1038. https://doi.org/10.1007/s13726-015-0390-8
[17] Sedghi, R.; Shaabani, A. Electrospun Biocompatible Core/Shell Polymer-Free Core Structure Nanofibers with Superior Antimicrobial Potency Against Multi Drug Resistance Organisms. *Polymer* **2016**, *101*, 151-157. https://doi.org/10.1016/j.polymer.2016.08.060
[18] Stepanyan, R.; Subbotin, A.V.; Cuperus, L.; Boonen, P.; Dorschu, M.; Oosterlinck, F.; Bulters, M.J.H. Nanofiber Diameter in Electrospinning of Polymer Solutions: Model and Experiment. *Polymer* **2016**, *97*, 428-439. https://doi.org/10.1016/j.polymer.2016.05.045
[19] McCann, J.T.; Marquez, M.; Xia, Y. Melt Coaxial Electrospinning: A Versatile Method for the Encapsulation of Solid Materials and Fabrication of Phase Change Nanofibers. *Nano Lett*. **2006**, *12*, 2868-2872. https://doi.org/10.1021/nl0620839
[20] Chen, C.; Wang, L.; Huang, Y. Morphology and Thermal Properties of Electrospun Fatty Acids/Polyethylene Terephthalate Composite Fibers as Novel Form-Stable Phase Change Materials. *Sol. Energy Mater. Sol. Cells* **2008**, *92*, 1382-1387. https://doi.org/10.1016/j.solmat.2008.05.013
[21] Pérez-Masiá, R.; López-Rubio, A.; Lagarón, J.M. Development of Zein-Based Heat-Management Structures for Smart Food Packaging. *Food Hydrocoll*. **2013**, *30*, 182-191. https://doi.org/10.1016/j.foodhyd.2012.05.010
[22] Kulkarni, A.; Bambole, V.A.; Mahanwar, P.A. Electrospinning of Polymers, Their Modeling and Applications. *Polym. Plast. Technol. Eng*. **2010**, *49*, 427-441. https://doi.org/10.1080/03602550903414019
[23] Saeed, M.J.; Azizli, K.; Isa, M.H.; Bashir, M.J.K. Application of CCD in RSM to Obtain Optimize Treatment of POME Using Fenton Oxidation Process. *J. Water Process. Eng*. **2015**, *8*, e7-e16. https://doi.org/10.1016/j.jwpe.2014.11.001
[24] Bezerra, M.A.; Santelli, R.E.; Oliveira, E.P.; Villar, L.S.; Escaleira, L.A. Response Surface Methodology (RSM) as a Tool for Optimization in Analytical Chemistry. *Talanta* **2008**, *76*, 965-977. https://doi.org/10.1016/j.talanta.2008.05.019
[25] Montgomery, D.C. *Design and Analysis of Experiments*; John Wiley and Sons, Inc.: Arizona, 2011.
[26] Hafizi, A.; Ahmadpour, A.; Koolivand-Salooki, M.; Koolivand- Salooki, M.; Heravi, M.M.; Bamoharram, F.F. Comparison of RSM and ANN for the Investigation of Linear Alkylbenzene Synthesis over $H_{14}[NaP_5W_{30}O_{110}]/SiO_2$ Catalyst. *J. Ind. Eng. Chem*. **2013**, *19*, 1981-1989. https://doi.org/10.1016/j.jiec.2013.03.007
[27] Chen, C.; Liu, W.; Yang, H.; Zhao, Y.; Liu, S. Synthesis of Solid–Solid Phase Change Material for Thermal Energy Storage by Crosslinking of Polyethylene Glycol with Poly (Glycidyl Methacrylate). *Sol. Energy* **2011**, *85*, 2679-2685. https://doi.org/10.1016/j.solener.2011.08.002
[28] Sarı, A.; Alkan, C.; Biçer, A. Synthesis and Thermal Properties of Polystyrene-Graft-PEG Copolymers as New Kinds of Solid–Solid Phase Change Materials for Thermal Energy Storage. *Mater. Chem. Phys*. **2012**, *133*, 87-94. https://doi.org/10.1016/j.matchemphys.2011.12.056
[29] Dang, T.N.; Nguyen, T.T.T.; Chung, O.H.; Park, J.S. Fabrication of Form-Stable Poly(ethylene glycol)-Loaded Poly(vinylidene fluoride) Nanofibers via Single and Coaxial Electrospinning. *Macromol. Res*. **2015**, *23*, 819-829. https://doi.org/10.1007/s13233-015-3109-y

[30] Nguyen, T.T.T.; Park, J.S. Fabrication of Electrospun Nonwoven Mats of Polyvinylidene Fluoride/Polyethylene Glycol/Fumed Silica for Use as Energy Storage Materials. *J. Appl. Polym. Sci*. **2011**, *121*, 3596-3603. https://doi.org/10.1002/app.34148
[31] Babapoor, A.; Karimi, G.; Khorram, M. Fabrication and Characterization of Nanofiber-Nanoparticle-Composites with Phase Change Materials by Electrospinning. *Appl. Therm. Eng*. **2016**, *99*, 1225-1235. https://doi.org/10.1016/j.applthermaleng.2016.02.026
[32] Babapoor, A.; Karimi, G.; Golestaneh, S.I.; Mezjin, M.A. Coaxial Electro-Spun PEG/PA6 Composite Fibers: Fabrication and Characterization. *Appl. Therm. Eng*. **2017**, *118*, 398-407. https://doi.org/10.1016/j.applthermaleng.2017.02.119
[33] Shi, Q.; Liu, Z.; Jin, X.; Shen, Y.; Liu, Y. Electrospun Fibers Based on Polyvinyl Pyrrolidone/Eu-polyethylene Glycol as Phase Change Luminescence Materials. *Mater. Lett*. **2015**, *147*, 113-115. https://doi.org/10.1016/j.matlet.2015.02.040
[34] Noshadi, I.; Amin, N.A.S.; Parnas, R.S. Continuous Production of Biodiesel from Waste Cooking Oil in a Reactive Distillation Column Catalyzed by Solid Heteropolyacid: Optimization Using Response Surface Methodology (RSM). *Fuel* **2012**, *94*, 156-164. https://doi.org/10.1016/j.fuel.2011.10.018
[35] Hafizi, A.;Ahmadpour, A.; Heravi, M.M.; Bamoharram, F.F.; Khosroshahi, M. Alkylation of Benzene with 1-Decene Using Silica Supported Preyssler Heteropoly Acid: Statistical Design with Response Surface Methodology. *Chinese J. Catal*. **2012**, *33*, 494-501. https://doi.org/10.1016/S1872-2067(11)60357-4
[36] Forutan, H.R.; Karimi, E.; Hafizi, A.; Rahimpour, M.R.; Keshavarz, P. Expert Representation Chemical Looping Reforming: A Comparative Study of Fe, Mn, Co and Cu as Oxygen Carriers Supported on $Al_2O_3$. *J. Ind. Eng. Chem*. **2015**, *21*, 900-911. https://doi.org/10.1016/j.jiec.2014.04.031
[37] Aliabadi, M.; Irani, M.; Ismaeili, J.; Najafzadeh, S. Design and Evaluation of Chitosan/Hydroxyapatite Composite Nanofiber Membrane for the Removal of Heavy Metal Ions from Aqueous Solution. *J. Taiwan Inst. Chem. Eng*. **2014**, *45*, 518-526. https://doi.org/10.1016/j.jtice.2013.04.016
[38] Chen, C.; Wang, L.; Huang, Y. Electrospun Phase Change Fibers Based on Polyethylene Glycol/cellulose Acetate Blends. *Appl. Energy* **2011**, *88*, 3133-3139. https://doi.org/10.1016/j.apenergy.2011.02.026
[39] Šehić, A.; Tomšič, B.; Jerman, I.; Vasiljević, J.; Medved, J.; Simončič, B. Synergistic Inhibitory Action of P- and Si-containing Precursors in Sol–Gel Coatings on the Thermal Degradation of Polyamide 6. *Polym. Degrad. Stab*. **2016**, *128*, 245-252. https://doi.org/10.1016/j.polymdegradstab.2016.03.026
[40] Wu, Q.; Lü, J.; Qu, B. Preparation and Characterization of Microcapsulated Red Phosphorus and its Flame-Retardant Mechanism in Halogen-Free Flame Retardant Polyolefins. *Polym. Int*. **2003**, *52*, 1326-1331. https://doi.org/10.1002/pi.1115

*Received: December 15, 2020 / Revised: February 12, 2021 / Accepted: May 12, 2021*

## ОПТИМІЗОВАНИЙ ДИЗАЙН ТА ОДЕРЖАННЯ ПОЛІЕТИЛЕНГЛІКОЛЬ 1000/ПОЛІАМІД 6 (PEG1000/PA6) НАНОВОЛОКОН ЯК МАТЕРІАЛІВ З ФАЗОВИМ ПЕРЕХОДОМ (PCMs)

***Анотація.*** *Ультрадисперсні нановолокна з фазовим переходом на основі поліетиленгліколю 1000 (PEG1000) як матеріалу з фазовим переходом (PCM) та поліаміду 6 (PA6) як допоміжного матеріалу виготовлено методом однонаправленого електроспінінгу на систематизованій основі, запланованій програмним забезпеченням Design-Expert®. Застосовано метод поверхневого відгуку (RSM) для оптимізації параметрів та умов, що ведуть до мінімізації діаметра волокна. За допомогою центрального композиційного плану (CCD) вивчено вплив вмісту PEG, прикладеної напруги, калібра голки та швидкості потоку на характеристики волокна. Згідно з розрахунками за квадратичною моделлю, мінімальний діаметр нановолокон становить 64,33 нм; фактичний діаметр волокон, виготовлених за оптимальних умов, показав дуже низьку відносну стандартну похибку (RSE). Встановлено, що масове співвідношення PEG/ PA6 найбільше впливає на діаметр волокон. Результати FTIR та FE-SEM підтвердили інкапсуляцію PEG у PA6, і відсутність змін у морфології після тестів на нагрівання. Для подальшого дослідження морфологічної структури та якості інкапсуляції PEG1000 у матрицях PA6 композиційні волокна оброблено розчинником з використанням етанолу. Запропоновано новий інноваційний метод контролю умов електроспінінгу для інкапсуляції матеріалів з фазовим переходом у полімерних матрицях, що дуже важливо у програмах енергозбереження/енерговідновлення.*

***Ключові слова:*** *електроспінінг, матеріал з фазовим переходом (PCM), метод поверхневого відгуку (RSM), поліетиленгліколь, поліамід 6.*